Supplemental Materials

Supplemental Table and Figure Legends

Supplemental Table 1

Summary of the quantifications for normalized immunofluorescence, ventral commissure, ventral funiculus, lateral funiculus thickness taken from all genetically altered mouse lines and their respective controls analyzed in this study. Values are represented as the means ±SEM from 5-8 sections and average among 4-5 animals/genotype.

Supplemental Figure 1. Specific Plexin-A1 protein is localized to dorsal spinal commissural neurons.

(A) A wild type (top row) and a *Plexin-A1*$^{-/-}$ (bottom row) transverse section from E11.5 mouse spinal cords co-labeled with antibodies that recognized a peptide corresponding to human (h)Plexin-A1 aa 182-200 (green; Abcam) and TAG1 (red) in commissural axons. **(B)** A *Plexin-A1*$^{-/-}$ spinal cord section at E11.5 co-labeled using antibodies against the most c-terminus 16 aa of mouse (m)Plexin-A1 (Yoshida et al., 2006) and TAG1 (red). Scale bar in A = 160 μm for both A and B. **(C-D)** Open-book spinal cord preparations of E11.5 mouse spinal cords taken from *Nrp2*$^{f/f;}$*FoxA2*$^{+/creERT2}$ embryos treated with tamoxifen (+TM)**(C)** or no TM **(D)**. Sections were processed by immunohistochemistry with anti-Nrp2 and anti-hPlxnA1. White arrows point to overlapping regions of the pre-crossing axons expressing PlxnA1 and Nrp2. FP, floor plate. Scale Bar, 50 μm in D for C and D.

Supplemental Figure 2. Post-crossing axons are sensitive to both Sema3B and Sema3F inhibition in vitro.

(A) Schematic diagram illustrating how post-crossing axon versus pre-crossing axon spinal cord explants are isolated. Representative micrograph illustrating an entire post-crossing axon spinal cord explant with neurite growing out from the ventral side, with the floor plate attached. **(B)** Representative images of spinal cord explants, on the ventral side, illustrating post-crossing axons treated with increasing Sema3B ligand concentrations. Three independent explant cultures are shown. **(C)**. Spinal cord explants containing post-crossing axons treated with either Sema3F or Sema3A at 1.0µg/ml. **(D)** Quantification of the mean neurite length taken from the explants treated with different Sema3 ligands and concentrations. N=4 independent explant cultures per ligand treatment condition; One-way ANOVA, post-hoc Tukey test, *p<0.05; **p<0.01; ***p<0.001. Statistical significance was also found between the following groups: p<0.05 for Sema3B 0.5µg/ml, p<0.01 for Sema3B 1.0µg/ml, and p<0.001 for Sema3B 2µg/ml compared to Sema3B 0.25µg/ml; p<0.001 for Sema3B concentrations 0.05, 1.0 and 2.0µg/ml compared to Sema3A 1.0µg/ml; p<0.05 for Sema3F 1.0µg/ml compared to Sema3A 1.0µg/ml.

Supplemental Figure 3. Specific deletion of floor plate derived-Neuropilin-2 in *Nrp2$^{f/f;}$FoxA2$^{creERT2/creERT2}$* mouse embryos show pre-crossing guidance defects in Nrp2- and TAG1-positive axons.

(A-B) Representative confocal images of E11.5 mouse spinal cord sections taken from a *Nrp2$^{f/f}$;FoxA2-$^{+/creERT2}$* embryo with no tamoxifen (No TM) treatment **(A)** and

Nrp2$^{f/f}$;FoxA2$^{creERT2/creERT2}$ embryo with tamoxifen (+TM) treatment **(B)**. Transverse sections were processed for immunohistochemistry using antibodies against TAG1 (red), Nrp2 (blue) and GFP (green). Scale bar, 160 μm in B for A and B. **(C-D)** Representative confocal images of E11.5 mouse spinal cord open-book preparations taken from an *Nrp2$^{f/f}$;FoxA2$^{+/+}$*(no cre), +TM **(C)** or *Nrp2$^{f/f}$;FoxA2$^{+/CreERT2}$*, +TM embryo **(D)**. The open-book was processed with anti-GFP (top panels) and anti-Nrp2 (bottom panels). GFP signal in the floor plate region indicates successful Cre mediate recombination in the *Nrp2$^{f/f}$;FoxA2$^{+/CreERT2}$*, +TM animal. While the ventral commissure in the *Nrp2$^{f/f}$;FoxA2$^{+/CreERT2}$*, +TM mutant appeared to contain fewer Nrp2-positive axons, similar Nrp2 fluorescent intensity was detected in the dorsal spinal cord, where the cell bodies of the commissural neurons are located, as indicated by the white dashed lines between the mutant and control. Scale bar, 50 μm in D for C and D.

Supplemental Figure 4. Deletion of floor plate-derived Neuropilin 2 does not alter the number of apoptotic cells or the cellular architecture of the mouse developing spinal cord in vivo.

Representative confocal images of E11.5 mouse spinal cords taken from *Nrp2$^{f/f}$;FoxA2$^{+/creERT2}$* and *Nrp2$^{f/f}$;FoxA2$^{creERT2/creERT2}$* embryos treated with tamoxifen (+TM) or without tamoxifen (No TM). TUNEL assay revealed no observable differences in the number of apoptotic cells between *Nrp2$^{f/f}$;FoxA2$^{+/creERT2}$* and *Nrp2$^{f/f}$;FoxA2$^{creERT2/creERT2}$* embryos treated with or without tamoxifen. Note, fluorescent signal detected in the floor plate is the endogenous GFP signal from only

animals treated with TM, indicated successful Cre mediate recombination specific to the floor plate cells. Positive control spinal cord section was treated with DNAse I to induce DNA fragmentation. Scale bar, 50 μm.

Supplemental Figure 5. Specific deletion of floor plate derived-Neuropilin-2 altered pre-crossing axon pathfinding in ventral GABAergic commissural neurons. **(A-B)** Representative confocal images of E11.5 mouse spinal cord sections from a *Nrp2$^{f/f}$;FoxA2$^{+/creERT2}$* embryo with no tamoxifen (No TM) treatment **(A)** and *Nrp2$^{f/f}$;FoxA2$^{+/creERT2}$* embryo with tamoxifen (+TM) treatment **(B)** processed for immunohistochemistry for GAD65 (blue), Nrp2 (red) and GFP (green). White arrows and white arrowheads point to GAD65+ and Nrp2+ axons, respectively. FP, floor plate. Scale bar for A and B left columns (low magnification), 160 μm; A and B right columns (high magnification), 80 μm. **(C)** Quantifications of GAD65 normalized fluorescence from *Nrp2 $^{f/f}$;FoxA2$^{+/creERT2}$* No TM and *Nrp2$^{f/f}$;FoxA2$^{+/creERT2}$* +TM embryos. Data are means ± SEM from 5-8 sections per embryo, where n=3 embryos per genotype; Student's *t*-test; *p<0.05. **(D)** Schematic diagram illustrating the parameters for the measurement of the normalized ventral and lateral funiculi. Measurements for the ventral funiculus (VF) and lateral funiculus (LF) are taken as indicated by the 'red bars' and normalized to the entire length of the dorsoventral axis of the spinal cord sections. The black diagonal and horizontal lines form a 45 degrees angle that demarcates the VF and LF. Similar measurement was performed for the ventral commissure (VC) normalized thickness. **(E)** Quantifications of normalized thickness of the ventral commissure (VC), ventral funiculus (VF) and

lateral funiculus (LF) from GAD65 labeled *Nrp2$^{f/f}$;FoxA2$^{+/creERT2}$* No TM (VF=0.078±.0042; LF=0.025±0.0021), and *Nrp2$^{f/f}$;FoxA2$^{+/creERT2}$* +TM (VF=0.049±0.0048; LF=0.013±0.0013) embryos. Data are means ± SEM from 5-6 sections measured per embryos, where n=3 embryos per genotype. ANOVA followed by post-hoc Tukey test, *p<0.05 compared to *Npr2$^{f/f}$;FoxA2$^{+/creERT2}$* No TM.

Supplemental Figure 6. Specific deletion of *Plexin-A1* in dorsal commissural neurons shows normal pre-crossing, but altered post-crossing, axon guidance. **(A-C)** Representative confocal micrographs of E11.5 mouse spinal cord sections taken from a *PlxnA1$^{+/+}$;Math1-Cre+-GFP* **(A)**, *PlxnA1$^{+/f}$;Math1-Cre+-GFP* **(B)**, and *PlxnA1$^{f/f}$;Math1-Cre+-GFP* littermate embryos **(C)**. All transverse sections were processed for immunocytochemistry for PlxnA1 (blue), Robo3.1 (red), and GFP (green). Scale bar for A and B, 225 μm. **(D)** Quantifications of normalized fluorescence in Robo3.1-positive pre-crossing axons showed no significant difference between littermates with the following genotypes: *PlxnA1$^{+/+}$;Math1-Cre+*, *PlxnA1$^{+/f}$;Math1-Cre+-GFP*, and *PlxnA1$^{f/f}$;Math1-Cre+-GFP*. Data are means ± SEM from 5-10 sections measured per embryos, where n=5 *PlxnA1$^{+/+}$;Math1-Cre+*; n=4 *PlxnA1$^{+/f}$;Math1-Cre-GFP+*; n= 3 *PlxnA1$^{f/f}$;Math1-Cre+-GFP*. ANOVA, not significant. **(E)** Quantifications of normalized thickness of the ventral commissure (VC), ventral funiculus (VF) and lateral funiculus (LF) from PlxnA1 labeled *PlxnA1$^{+/+}$;Math1-Cre+*; *PlxnA1$^{+/f}$;Math1-Cre+-GFP*; and *PlxnA1$^{f/f}$;Math1-Cre+-GFP* embryos. Data are means ± SEM from 6-8 sections measured per embryos, where n=3 *PlxnA1$^{+/+}$;Math1-Cre+*; and n=5 *PlxnA1$^{+/f}$;Math1-Cre+-GFP*; *PlxnA1$^{f/f}$;Math1-Cre+-GFP* embryos. ANOVA

followed by post-hoc Tukey test, *p<0.05 compared to *PlxnA1$^{+/+}$;Math1-cre+*. **(F)** Schematic diagram illustrating wild type (left) and axonal deletion of PlxnA1 (right) genotypes and phenotypes observed in E11.5 spinal cords.

Supplemental Figure 7. Plexin-A1 null mutant embryos have normal pre-crossing axonal pathfinding.

(A-B) Confocal images show E11.5 wild type mouse spinal cord **(A)** and Plexin-A1 homozygote null mutant (*PlxnA1$^{-/-}$*) spinal cord **(B)**. Both sections were processed for immunohistochemistry for Nrp2 (red), Robo3.1 (blue) and TAG1 (green). Scale bar, 160 μm.

Genotype	Normalized Fluorescence				Normalized Ventral Commissure Thickness				Normalized Ventral Funiculus Thickness		Normalized Lateral Funiculus Thickness	
	Nrp2	Robo3.1	TAG1	GAD65	Nrp2	Robo3.1	GAD65	PlexinA1	GAD65	PlexinA1	GAD65	PlexinA1
Nrp2$^{f/f}$;FoxA2$^{+/CreERT2}$ (No TM)	11.89 ± 0.72	11.57 ± 0.57	3.26 ± 0.37	14.48± 1.06	0.0614 ± 0.0015	0.047 ± 0.0015	0.056 ± 0.0021	-	0.078 ± 0.0042	-	0.025 ± 0.0021	-
Nrp2$^{f/f}$;FoxA2$^{+/CreERT2}$ (+TM)	7.52 ± 0.50*	8.87 ± 0.51*	1.38 ± 0.14*	7.66 ± 1.20*	0.0452 ± 0.0022*	0.033 ± 0.0021*	0.040 ± 0.0032*	-	0.049 ± 0.0048*	-	0.013 ± 0.0013*	-
Nrp2$^{f/f}$;FoxA2$^{CreERT2/CreERT2}$ (+TM)	8.16 ± 0.50*	-	1.86 ± 0.16*	-	0.0243 ± 0.0014*	0.016 ± 0.0011*	-	-	-	-	-	-
Nrp2$^{+/f}$;Math1-Cre^{+}	-	7.48 ± 0.42	-	-	-	-	-	-	-	-	-	-
Nrp2$^{f/f}$;Math1:Cre^{+}	-	7.97 ± 0.69	-	-	-	-	-	-	-	-	-	-
PlxnA1$^{+/+}$;Math1-Cre^{+}	-	5.48 ± 0.39	-	-	-	-	-	0.0793 ± 0.0027	-	0.0886 ± 0.0031	-	0.0315 ± 0.0017
PlxnA1$^{+/f}$;Math1-Cre^{+}	-	5.65 ± 0.32	-	-	-	-	-	0.05392± 0.0045*	-	0.0724 ± 0.0033*	-	0248 ± 0.0019
PlxnA1$^{f/f}$;Math1-Cre^{+}	-	6.47 ± 0.4	-	-	-	-	-	0.0626 ± 0.0018*	-	0.0693 ± 0.0013*	-	0.0206 ± 0.0009
Nrp2$^{+/f}$;FoxA2$^{+/+}$;PlxnA1$^{+/-}$(+TM)	-	4.78 ± 0.28	-	-	-	0.0640 ± 0.002	-	-	-	-	-	-
Nrp2$^{f/f}$;FoxA2$^{+/CreERT2}$;PlxnA1$^{+/+}$(+TM)	-	3.30 ± 0.3 *	-	-	-	0.0511 ± 0.001*	-	-	-	-	-	-
Nrp2$^{f/f}$;FoxA2$^{CreERT2/CreERT2}$;PlxnA1$^{-/-}$ (+TM)	-	5.73 ± 0.44	-	-	-	0.0455 ± 0.002*	-	-	-	-	-	-

*Statistical significance compared to respective controls

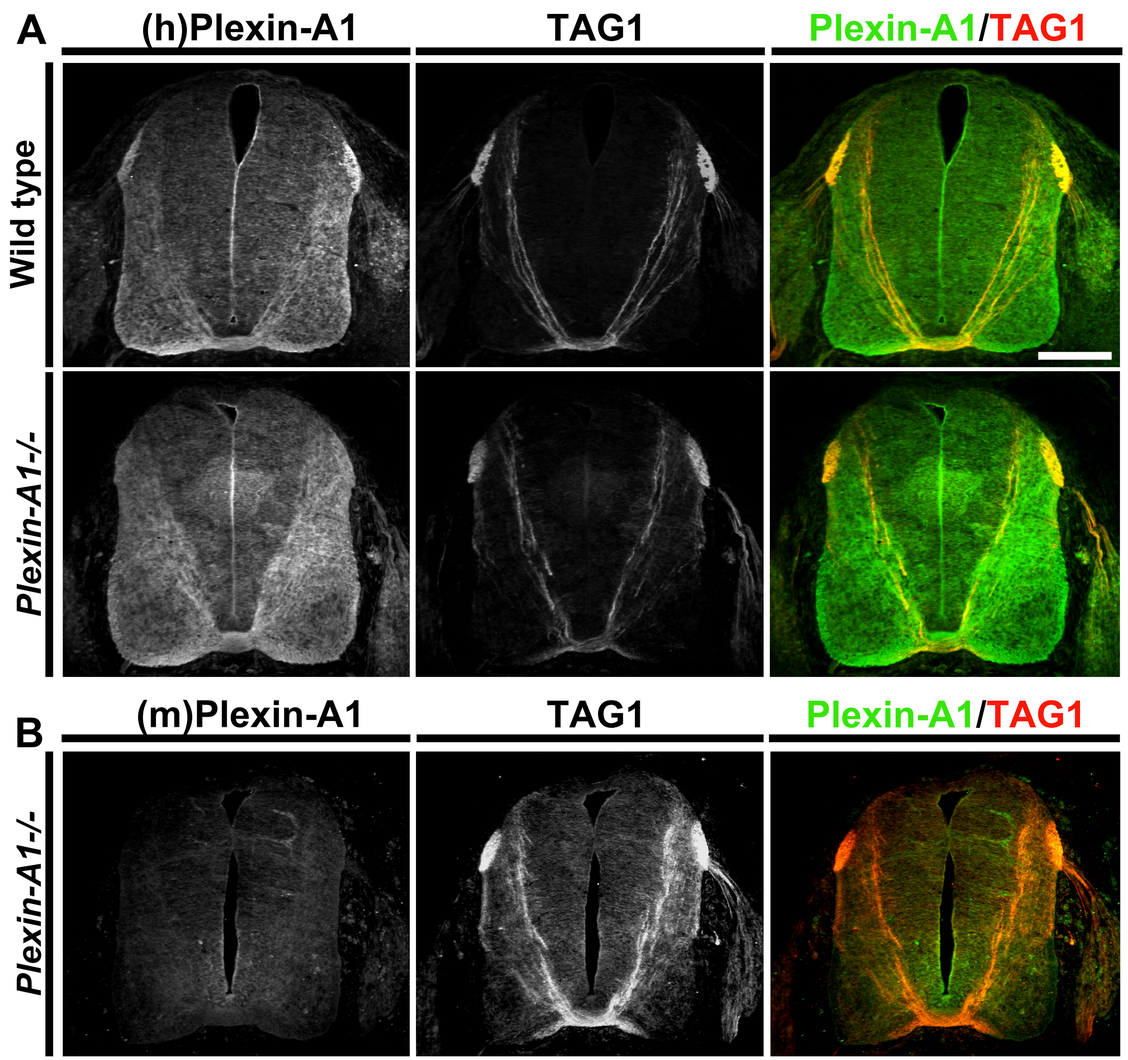
A
(h)Plexin-A1
TAG1
Plexin-A1/TAG1
Wild type
Plexin-A1-/-
B
(m)Plexin-A1
TAG1
Plexin-A1/TAG1
Plexin-A1-/-

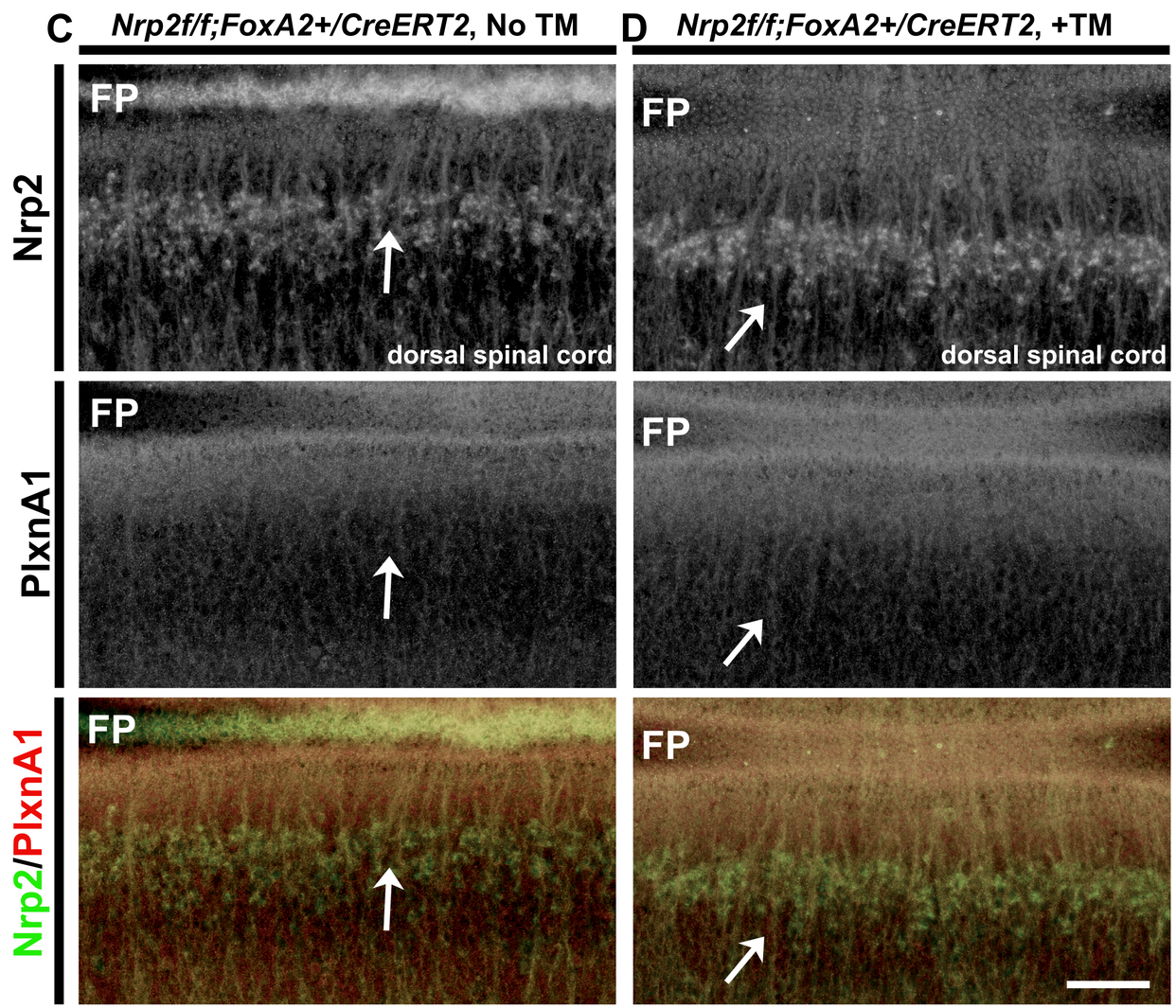
C
Nrp2f/f;FoxA2+/CreERT2, No TM
D
Nrp2f/f;FoxA2+/CreERT2, +TM
Nrp2
PlxnA1
Nrp2/PlxnA1
FP
dorsal spinal cord

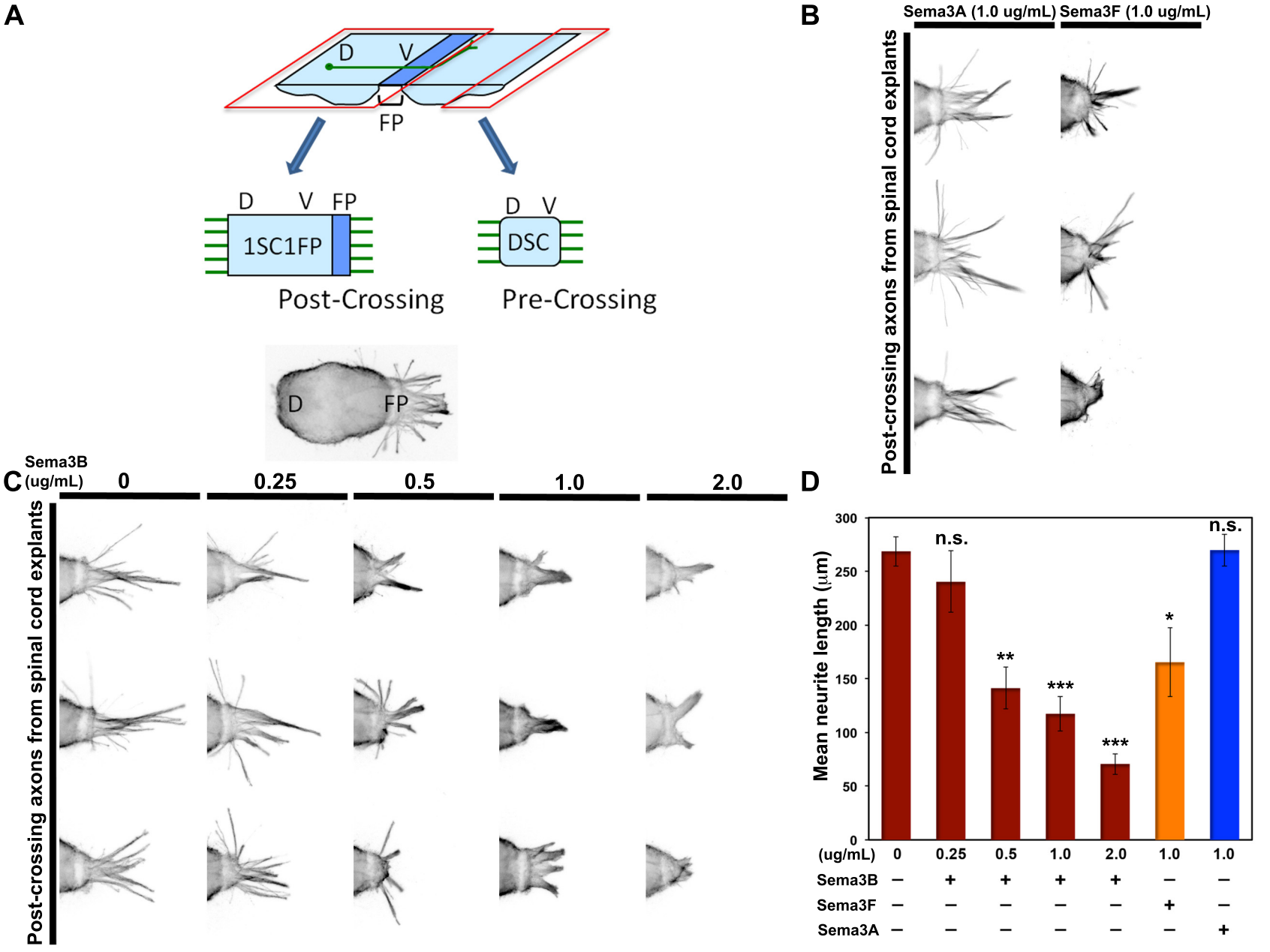
A
D
V
FP
D V FP
1SC1FP
D V
DSC
Post-Crossing
Pre-Crossing
D
FP
B
Sema3A (1.0 ug/mL)
Sema3F (1.0 ug/mL)
Post-crossing axons from spinal cord explants
C
Sema3B (ug/mL)
0
0.25
0.5
1.0
2.0
Post-crossing axons from spinal cord explants
D
Mean neurite length (μm)
300
250
200
150
100
50
0
n.s.
n.s.
**
***
***
*
(ug/mL) 0 0.25 0.5 1.0 2.0 1.0 1.0
Sema3B – + + + + – –
Sema3F – – – – – + –
Sema3A – – – – – – +

Hernandez-Enriquez_Supplemental Fig 3

A

Nrp2

TAG1

GFP

Nrp2/TAG1/GFP

Nrp2 f/f;FoxA2+/CreERT2, No TM

B

Nrp2 f/f;FoxA2CreERT2/CreERT2, +TM

C

Nrp2f/f;FoxA2+/+ (no cre), +TM

D

Nrp2f/f;FoxA2+/CreERT2, +TM

GFP

floor plate

Nrp2

ventral commissure

dorsal spinal cord

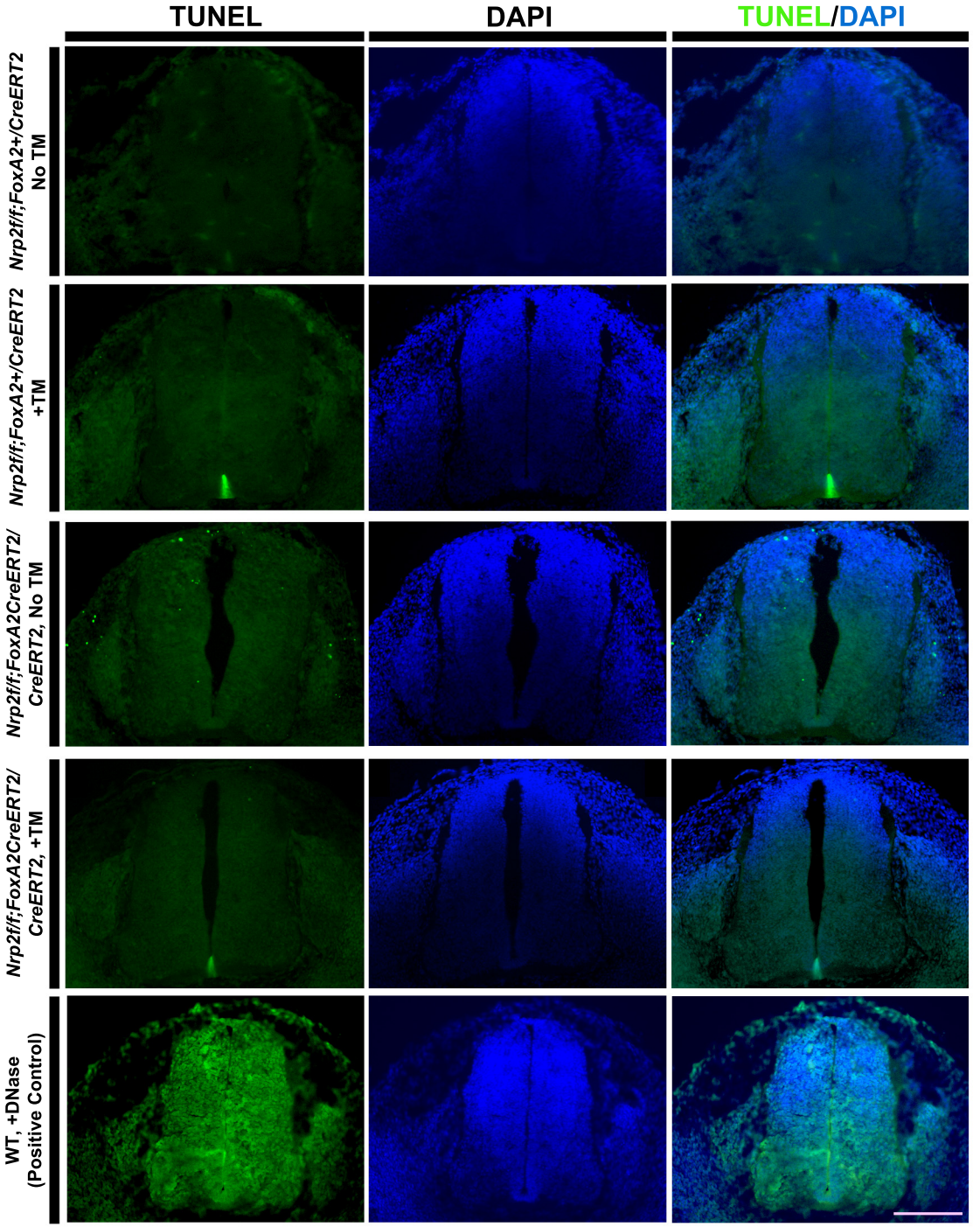
TUNEL
DAPI
TUNEL/DAPI
Nrp2f/f;FoxA2+/CreERT2 No TM
Nrp2f/f;FoxA2+/CreERT2 +TM
Nrp2f/f;FoxA2CreERT2/ CreERT2, No TM
Nrp2f/f;FoxA2CreERT2/ CreERT2, +TM
WT, +DNase (Positive Control)

Hernandez-Enriquez_Supplemental Fig 5

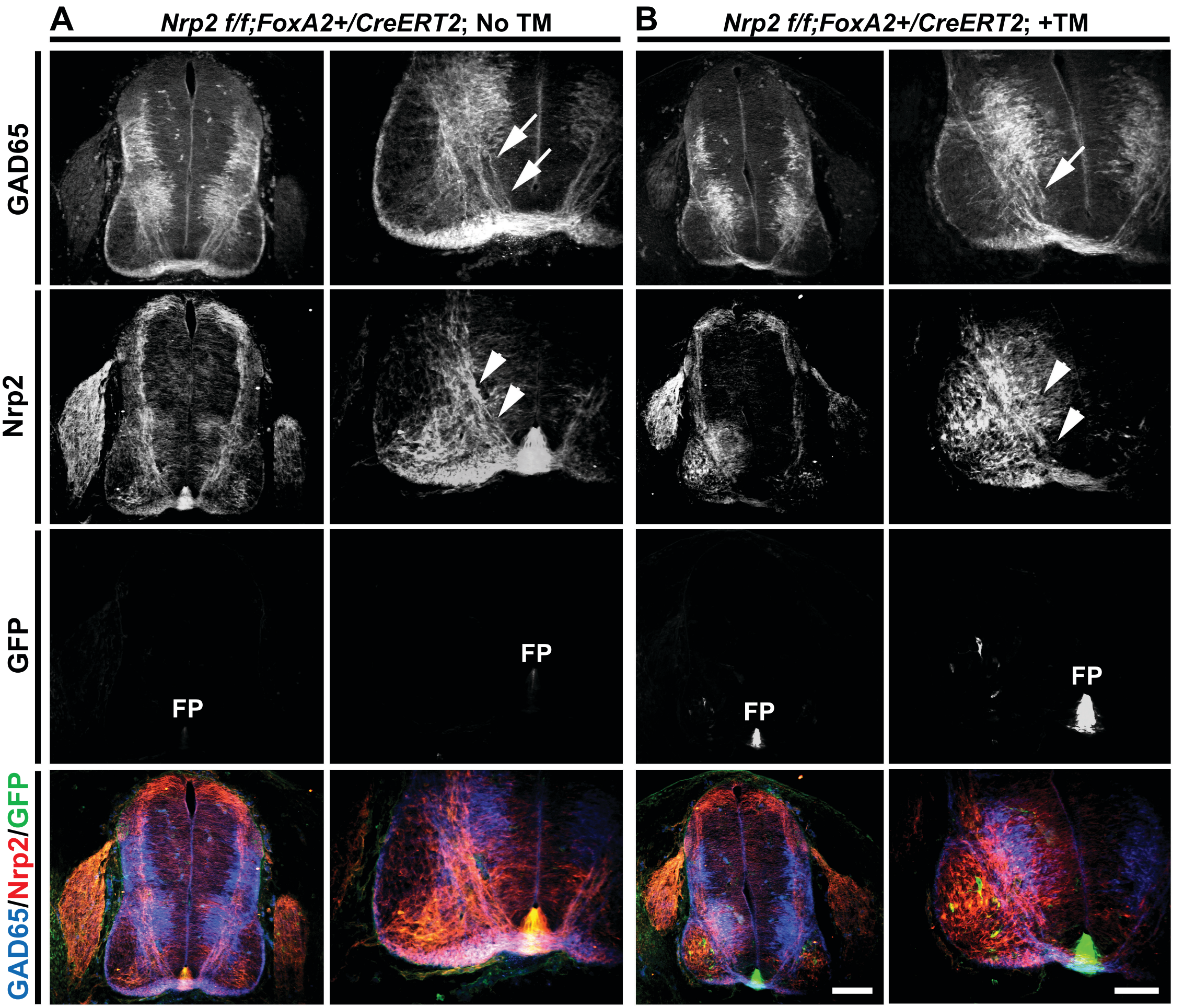

Hernandez-Enriquez_Supplemental Fig 6

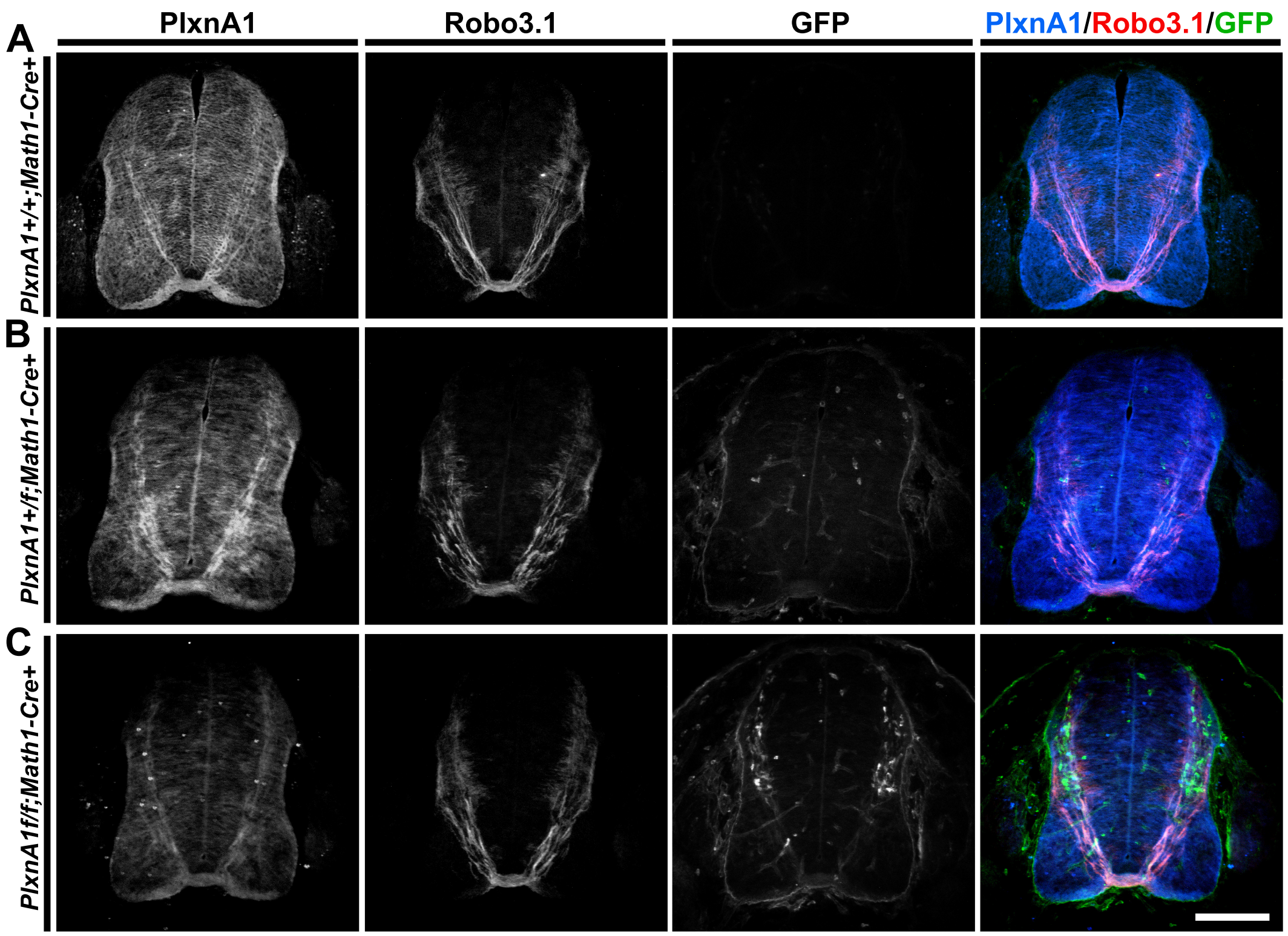

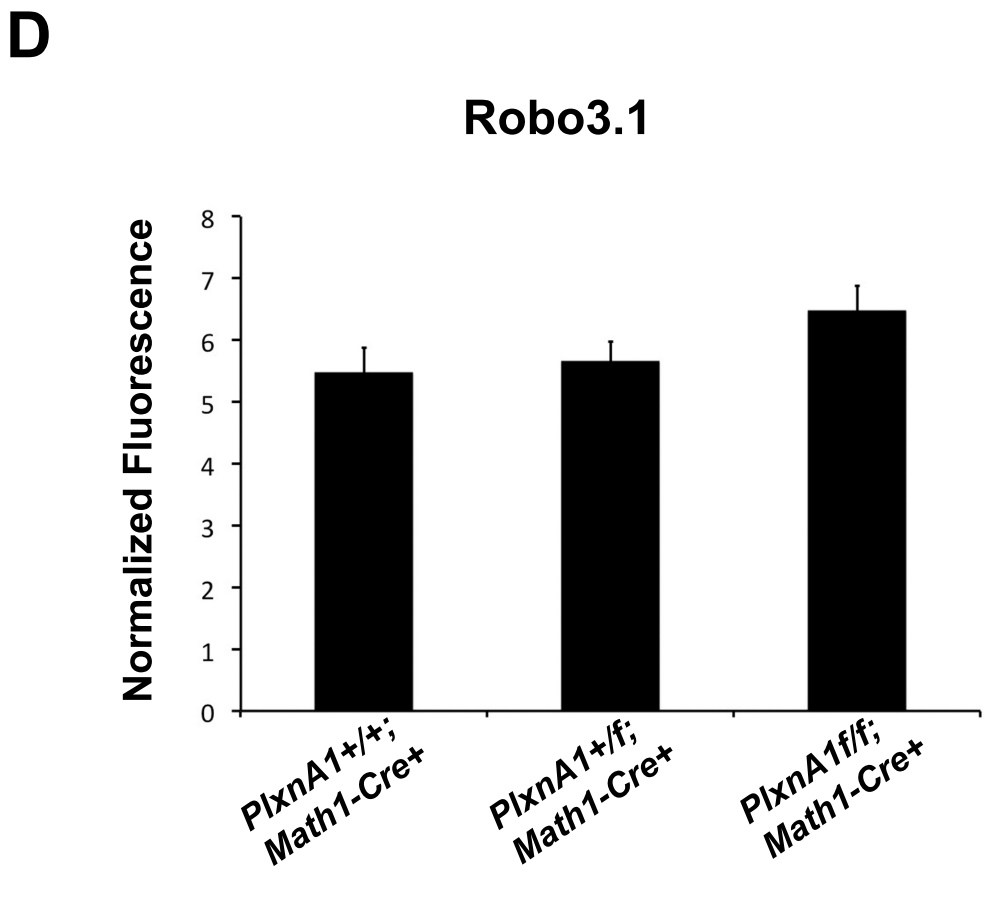

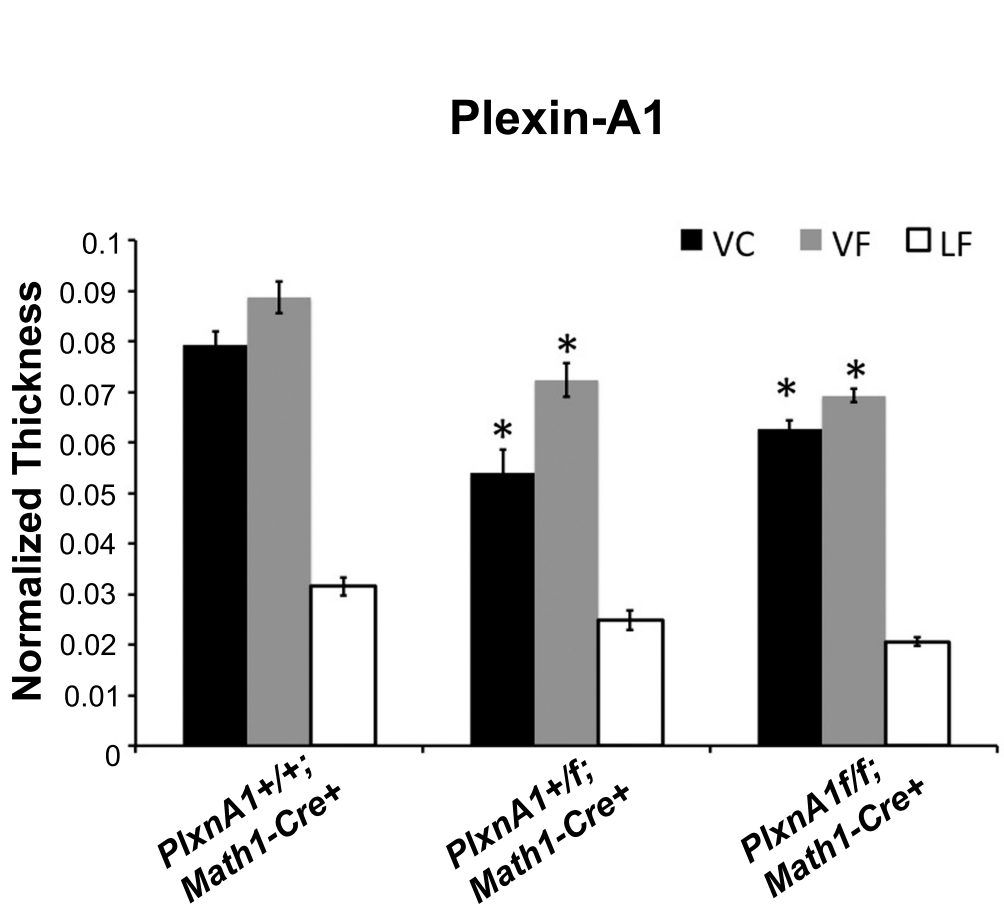

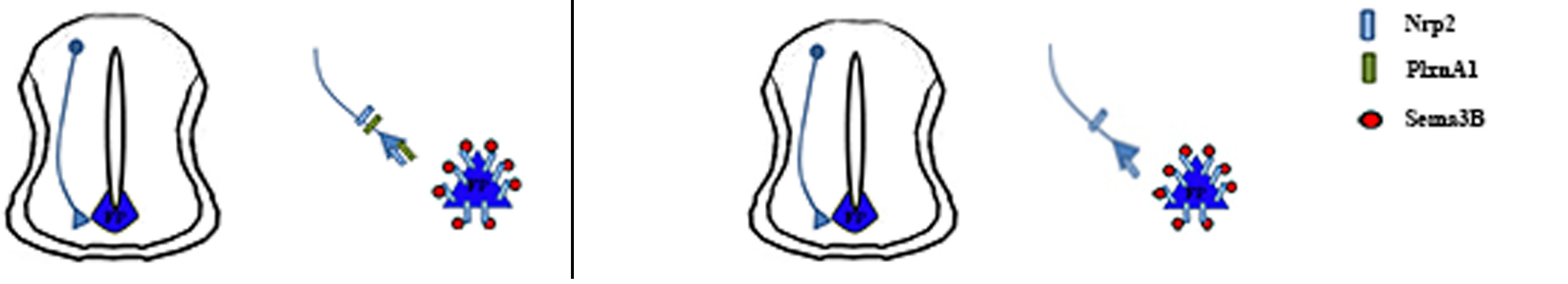

Hernandez-Enriquez_Supplemental Fig 7